Journal of
Synchrotron Radiation

ISSN 0909-0495

Received 7 September 2008
Accepted 5 April 2009

Portable multi-anvil device for *in situ* angle-dispersive synchrotron diffraction measurements at high pressure and temperature

Yann Le Godec,[a]* Gérard Hamel,[a] Vladimir L. Solozhenko,[b] Domingo Martinez-Garcia,[c] Julien Philippe,[a] Tahar Hammouda,[d] Mohamed Mezouar,[e] Wilson A. Crichton,[e] Guillaume Morard[e] and Stefan Klotz[a]

[a]IMPMC, Université Pierre et Marie Curie, 140 rue de Lourmel, 75015 Paris, France, [b]LPMTM-CNRS, Université Paris Nord, 99 avenue J. B. Clément, 93430 Villetaneuse, France, [c]DFA and ICMUV, Edificio Investigación, pl. 1, Dr Moliner 50, 46100 Burjassot, Valencia, Spain, [d]LMV, Université Blaize Pascal, 5 rue Kessler, 63038 Clermont-Ferrand, France, and [e]ESRF, 38000 Grenoble, France. E-mail: yann.legodec@impmc.jussieu.fr

A recently developed portable multi-anvil device for *in situ* angle-dispersive synchrotron diffraction studies at pressures up to 25 GPa and temperatures up to 2000 K is described. The system consists of a 450 ton V7 Paris–Edinburgh press combined with a Stony Brook 'T-cup' multi-anvil stage. Technical developments of the various modifications that were made to the initial device in order to adapt the latter to angular-dispersive X-ray diffraction experiments are fully described, followed by a presentation of some results obtained for various systems, which demonstrate the power of this technique and its potential for crystallographic studies. Such a compact large-volume set-up has a total mass of only 100 kg and can be readily used on most synchrotron radiation facilities. In particular, several advantages of this new set-up compared with conventional multi-anvil cells are discussed. Possibilities of extension of the (P, T) accessible domain and adaptation of this device to other *in situ* measurements are given.

Keywords: high pressure; high temperature; multi-anvil system; angle-dispersive X-ray diffraction.

1. Introduction

In situ structural studies under conditions of high pressure and high temperature (HP-HT) of materials are of equal interest to planetary scientists, materials scientists, physicists and chemists. This approach represents a powerful tool for better understanding some fundamental physical properties of condensed matter, such as, for example, crystal structure, equation of state, compressibility and phase transitions. Other research fields include the observation of chemical reactions between compounds under extreme conditions, materials synthesis [*e.g.* super-hard materials such as diamond or more recently BC_2N (Solozhenko *et al.*, 2001)] and crystal growth kinetics and mechanisms under HP-HT. Traditionally, one of the most popular techniques for such *in situ* studies is synchrotron powder diffraction, and many dedicated synchrotron beamlines throughout the world enable these studies.

Devices commonly used for such HP-HT studies can be separated into two broad classifications: diamond anvil cells and large-volume apparatus. Given that proper pressure-transmitting media are used, the two techniques give good hydrostatic conditions particularly at high temperature. Concerning P and T ranges, temperature monitoring and sample environment, each technique has advantages and limitations.

Diamond anvil cells [a short overview of the most important developments in diamond anvil cell techniques can be found by Brister (1997)] allow very high pressures (Mbar range) and temperatures (thousands of K using laser heating) to be achieved simultaneously. In addition, diamond anvil cells are portable (apart from the laser heating system), have optical windows to the sample (which permits Raman and Brillouin scattering, infrared absorption *etc.*) and are very simple to use. On the other hand, samples studied are of very small size (<100 μm wide, <50 μm thick) and, during laser heating, the sample chamber is submitted to very high temperature gradients. This can be problematic when studying multi-component systems where chemical separation occurs along thermal gradients. Thermal gradients also yield pressure gradients inside the sample chamber owing to thermal pressure effects. The problems associated with gradients are therefore a limiting factor for the studies of complex systems such as those of interest for materials and planetary sciences.

Multi-anvil presses [more details can be found by Huppertz (2004) who summarizes the history, the design and the calibration of various versions of multi-anvil devices] are of very common use in the Earth science community. They have been the workhorse for the construction of precise phase diagrams under conditions of the first 800 km inside our planet. The multi-anvil apparatus allows thermodynamic equilibrium to be achieved under controlled, known and independently determined pressure and temperature conditions. Independent monitoring of pressure and temperature permits wide P–T ranges to be scanned at high resolution (<0.5 GPa, 50 K). Conditions commonly achieved with multi-anvil presses range from 0.1 to 25 GPa, up to 2500 K. Recent advances using sintered diamond anvils allowed 69 GPa to be reached at room temperature and 44 GPa at 2100 K or 35 GPa at 2800 K (Ito *et al.*, 2004; Irifune, 2002; Kubo *et al.*, 2003). In addition, multi-anvil presses allow a run duration of several hours or days when necessary. Equilibrium phase compositions can be determined on recovered samples so that thermodynamic models can be constructed or refined. Actually, large sample quantities (several mm^3) can be treated with this equipment allowing the use of various analytical tools on recovered samples.

Developments at synchrotron facilities in Japan (Shimomura, 1984) and later in the USA led to the setting up of multi-anvil presses on dedicated beamlines. This allowed progress in studies on non-quenchable phases, reaction kinetics, viscosity and plasticity. These advances result from the combination of sample imagery (by absorption contrast) and energy-dispersive X-ray diffraction. Over the last decade these synchrotron facilities have been used with sintered diamond anvils and allowed to explore *in situ* phase relationships at very high pressure and temperature (Ito *et al.*, 2004; Irifune, 2002; Kubo *et al.*, 2003). Presently, multi-anvil presses installed on beamlines require the beamlines to be entirely (or at least to a great extent) devoted to that piece of equipment only. This is not a problem on its own because of the many types of experiments that can be achieved and the large number of groups interested in these investigations. However, owing to the nature of anvil material and their geometrical arrangement, multi-anvil applications are presently confined to white-beam set-ups which limits the accuracy of precise crystal structure determination and refinement of high-pressure phases, which demand high-quality diffraction patterns with reliable diffraction intensities. Another limitation of such multi-anvil presses is the time consumed for decompression (several hours). Because the press is positioned on the beam path, no other experiment can be done in the meantime which could be considered as a considerable waste of beam time.

As an alternative and a possible remedy to some of the limitations of the various systems discussed above, we have combined in an original set-up the miniaturized multi-anvil T-cup design of Stony Brook (Vaughan *et al.*, 1998) with a small-sized press of the Paris–Edinburgh type. One of the significant benefits of our set-up, compared with the previous methods, is that, with some modifications, it is easy to perform X-ray diffraction studies using the angular-dispersive mode and to avoid the wasting of beam time by the use of several presses simultaneously (see below).

In this paper, this new device is fully described and we report the various modifications that we had to make to our set-up in order to adapt the latter to angular-dispersive X-ray diffraction. A detailed description of the HP-HT X-ray diffraction experiments is given in the next section, followed by a presentation of some results conducted in various systems, which finally illustrate the efficiency of the set-up and the data quality that can be obtained. Possibilities of extension of the (P, T) accessible domain and the future adaptation of our new device to other *in situ* measurements are given as final prospects.

2. Description of the system

Our new HP-HT apparatus consists of a 450 ton large-volume Paris–Edinburgh press (V7) combined with a T-cup multi-anvil device (Vaughan *et al.*, 1998).

2.1. The Paris–Edinburgh press

The Paris–Edinburgh (PE) cell in its standard design is a compact large-volume press with a 250 ton capacity and a mass of only 50 kg. Originally developed for time-of-flight neutron scattering experiments at ISIS (Besson *et al.*, 1992), this press has been adapted later for a wide range of *in situ* HP-HT measurements such as neutron and X-ray diffraction, EXAFS, Compton scattering, inelastic neutron and X-ray scattering, and ultrasonic studies (Le Godec *et al.*, 2005, and references therein). In its standard configuration this press is capable of pressure in excess of 25 GPa (at room temperature) for neutron scattering experiments (Klotz *et al.*, 1995). For synchrotron use, this device, equipped with appropriate conical anvils, can generate static pressures up to 8 GPa and simultaneously temperatures up to 2200 K on several mm^3 sample volumes. Nevertheless, all current applications of the PE press are based an opposed anvils geometry. It is well known from experience that in such geometry the pressure and temperature range is necessary limited. To overcome these limitations, we recently designed a new high-pressure device for *in situ* X-ray diffraction studies using the V7 PE press (Le Godec *et al.*, 2005). The V7 (dimensions 24 × 24 × 41 cm) has a capacity of 450 ton, *i.e.* almost twice that of the standard PE presses, but still a mass of less than 100 kg. Moreover, the press can be easily dismounted in a few minutes for easier transport. Fig. 1 shows the assembled and disassembled V7 PE cell. In contrast with the usual PE cell where the oil pressure in the ram can be raised using a simple hand-operated hydraulic pump, our V7 cell has a more sophisticated system of compression. The pressure is generated by a computer-controlled hydraulic ('syringe') pump with a capacity of 50 cm^3 and 3000 bar (Sanchez Technologies, France). This device enables a very precise control of the rate of compression and decompression. It also allows automatic multiple reloads when the stroke of the pump is at the end, which is particularly useful during the download procedure

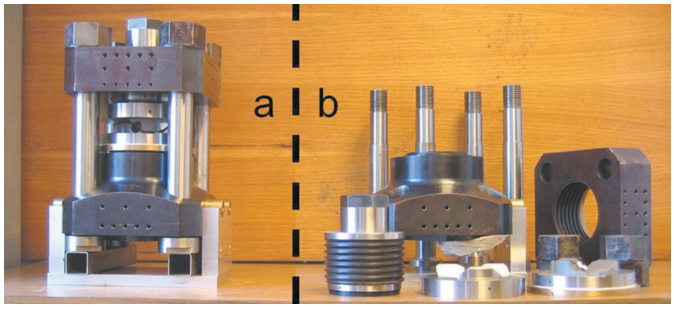

Figure 1
Assembled (*a*) and disassembled (*b*) V7 PE cell with the multi-anvil T-cup cell. The V7 has dimensions of 24 × 24 × 41 cm and a mass of less than 100 kg.

that can last several hours. The main advantage of the device is the possibility to program continuous and controlled pressure ramps and hence avoid the possible irregular increase (or decrease) of oil pressure observed when the hydraulic oil pressure is controlled manually. With this system, the occurrence of blow-outs has been found to be reduced, which shows that the performance of the system is very sensitive to the rate of compression or decompression.

2.2. The T-cup module

The T-cup module is a miniaturized KAWAI-type apparatus.[1] In this device, pressure is generated in two anvil stages. The first stage is a tool steel sphere split into six parts that form a central cubic cavity (23 mm on edge) which contains the second-stage anvils. The latter are equipped with eight cube-shaped inner anvils (10 mm edge length) made of tungsten carbide (WC) with a truncated edge length of 2.0 mm. The compression axis is along the [111] direction of the cubic cavity that is filled with the inner anvils. The truncated cubes, which enclose an octahedral cavity that contains the pressure cell, are separated from one another by compressible preformed crude pyrophyllite gaskets. The pressure medium is a 7 mm edge length octahedron made of a mixture of boron powder and epoxy resin (weight ratio 4:1) cold compressed at about 1.4 GPa. A cylindrical hole (2 mm in diameter) is drilled into this octahedron so as to accommodate a high cylindrical resistivity furnace (made of $LaCrO_3$), molybdenum discs, electrical contacts, ceramic insulator discs and a hexagonal boron nitride capsule. Generally, the sample under study is inserted inside this BN piece, crimped in a metal capsule (usually made of platinum or gold) in order to avoid chemical reactions with the environment of the sample under HP-HT conditions and also to recover it more easily. Heating of the sample is provided to the cell assembly by a DC power supply (0–200 A and 0–15 V) delivering an adjustable constant power input. A detailed description of the system and of its optimization by off-line tests is given by Le Godec *et al.* (2005). Fig. 2 shows the sample assembly most often used in our laboratory

[1] This name was proposed after its original designer, N. Kawaii (Kawaii & Endo, 1970). This apparatus is also referred to as '6–8 or MA8-type apparatus', as well as 'Walker-type apparatus' or 'split-sphere apparatus'.

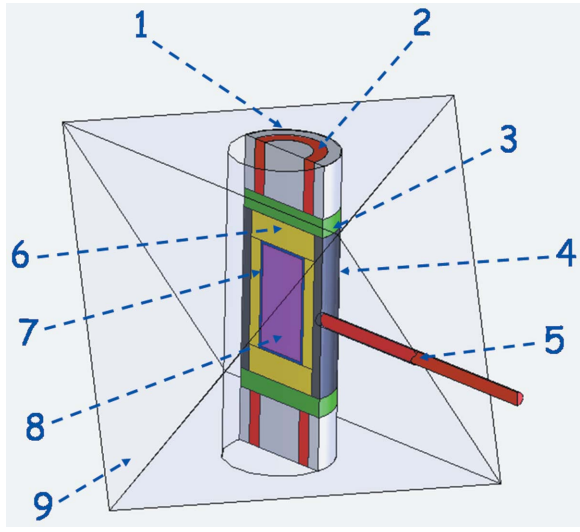

Figure 2
Sample assembly used for *ex situ* study. (1) Insulating ceramic. (2) Electrical contact. (3) Molybdenum disc. (4) Furnace ($LaCrO_3$). (5) Thermocouple. (6) Sample insulated capsule (usually MgO). (7) Metallic capsule (usually Pt or Au). (8) Sample. (9) Octahedron.

for *ex situ* synthesis. Using various precursors, we have attempted recently to synthesize new binary and ternary super-hard diamond-like phases in the B–C–N system at HP-HT. The recovered samples after HP-HT treatment have offered sufficient substance to all investigations necessary. For example, the structure and properties of our quenched samples have been analyzed by powder X-ray diffraction, Raman spectroscopy, hardness measurements, electron microscopy, electrical conductivity measurements, thermal analysis, electron energy-loss spectroscopy and Brillouin scattering (Solozhenko *et al.*, 2009).

3. Adaptation to angle-dispersive synchrotron X-ray diffraction

3.1. Insufficiency of *ex situ* studies

As already outlined in the previous section, our new *P–T* apparatus, after calibration of the pressure as a function of the hydraulic oil pressure (Le Godec *et al.*, 2005), has been used to synthesize new and useful materials not yet available by other means (Solozhenko *et al.*, 2009). This makes this portable apparatus suitable for synthesizing a sufficient amount of materials at HP-HT, and then returning this sample to ambient conditions before making a wide variety of characterization measurements. This approach is acceptable for identification of quenchable phase products, but will fail to give information about processes or structural data under extreme conditions. The alternative to such *ex situ* studies is of course *in situ* structural measurements such as *in situ* X-ray diffraction under extreme conditions. This probe is crucial since it yields direct structural data on HP-HT phases and provides a direct measurement of critical thermodynamic parameters and crystal structural changes as a function of pressure and temperature. In particular, such *in situ* synchrotron studies are

essential because they avoid reversibility processes in phase transitions and allow the true nature and kinetics of the process to be observed during its evolution. This is therefore the most suitable technique in geosciences to obtain the best detailed information about mineral crystal structures at simultaneous HP-HT and hence identify the materials which reside deep within the Earth. Moreover, it also represents a major advance for materials synthesis and crystal growth since it allows studies of the mechanism and kinetics of the phase transformations, and finally is crucial for finding the most interesting (P, T) 'route' to recover the materials synthesized under extreme conditions [especially to lower the (P, T) conditions of synthesis (Le Godec *et al.*, 2008)].

3.2. *In situ* synchrotron diffraction studies using multi-anvil cells

Many synchrotron beamlines throughout the world enable *in situ* synchrotron diffraction studies using multi-anvil cells, starting in Japan at the Photon Factory (Tsukuba) with MAX80 (MAX80 stands for 'multi-anvil X-ray apparatus designed in 1980'), MAX90 (designed in 1990) and Stony Brook (USA) with SAM85 (six anvil machine designed in 1985). Nevertheless, in these apparatuses, limited X-ray access imposes some limits on the quality of the crystallographic data that can be obtained. In these multi-anvil cells, the incident X-ray beam usually passes through the gaps between the WC cubes of the eight-cube assembly and diffracts through gaps between the first-stage anvils. As a result, HP-HT large-volume studies are often limited to the energy-dispersive X-ray diffraction technique (EDX), where measurement is made over photon energy E at a fixed 2θ angle. This popular technique is very effective because it features rapid data collection (of the order of minutes or seconds) and real-time display of the accumulating spectrum on a multichannel analyzer. Moreover, this technique has the advantage that the incident and diffracted beams can be well collimated in order to eliminate the contamination of the pressure-transmitting medium surrounding the sample. Hence, with such a diffraction geometry, clean diffraction patterns can easily be obtained, allowing compressibility studies, phase transformations investigations *etc.* Nevertheless, the EDX technique does not provide reliable crystal chemistry information, and complex high-pressure structures cannot usually be solved since Rietveld analysis requires high-accuracy intensity data to extract quantitative crystallographic information such as bonding characteristics and atomic positions of crystalline samples. Studies on liquid and/or amorphous structure are even more complicated because very accurate intensities would be required and the diffraction profile from a disordered system is usually broad and very weak in intensity compared with the signal of the sample environment. The diffracted signal needs, in that case, to be carefully corrected for the energy dependence of the brilliance of the X-ray source, for the response of the detector and for the energy dependence of the absorption of the sample which varies at high pressure and temperature. In practice, it is very difficult

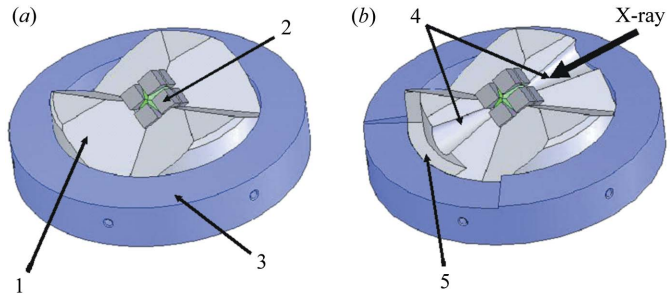

Figure 3
Schematic diagram of the initial T-cup module for *ex situ* studies (*a*) and the modified module for *in situ* X-ray diffraction studies (*b*). (1) First-stage anvils. (2) Second-stage anvils. (3) Containment ring. (4) Grooves for the incident and diffracted beam. (5) Grooves for the Sollers slit system.

or even impossible to precisely determine these corrections. Consequently, the only alternative[2] is the use of a monochromatic beam and hence of the angle-dispersive X-ray diffraction technique. However, contrary to EDX, the diffracted signal needs to be collimated at all 2θ angles simultaneously because of the two-dimensional nature of the detection. For this, a multi-slit system (also called a Sollers slit system) can be used, which consists of multiple slits that are in a radial alignment, centred at the sample. In this case the spatial selectivity operates simultaneously in the whole angular domain defined by the intersection of the detector area and the opening angle of the pressure cell. The volume seen by the detector is defined by the incident beam, the inner slit and the outer slit network dimensions. The main difficulty is the definition of the optimum geometry of the slit's network which is compatible with the machining limitations of a highly X-ray absorbing material (heavy metals) and the multi-anvil press dimensions and access in order to minimize this volume, *i.e.* to make the system as efficient as possible.

3.3. Modifications of our portable multi-anvil apparatus

Several modifications were necessary to adapt our portable multi-anvil apparatus to angular-dispersive X-ray diffraction. In the usual *ex situ* configuration depicted previously (see Figs. 2 and 3*a*), the first-stage anvils (made of hard steel), the eight WC cubes and finally the octahedron itself (because of the chromite heater) absorb the X-ray beam too much. Hence, the main issue in modifying the set-up to allow X-ray access to the sample is to remove the highly absorbing materials from the beam path while still maintaining the (P, T) performances of the apparatus.

3.3.1. Modifications of the first-stage anvils. Modifications of the first-stage anvils were carried out in the simplest possible way: by machining some grooves (see Fig. 3) into some parts of the first-stage anvils, X-rays diffracted at a 2θ

[2] In fact, a new diffraction technique combining angle- and energy-dispersive structural analysis and refinement (CAESAR) has been developed (Wang *et al.*, 2004). If this new technique is very useful in many cases, it should be noted that the data processing is quite complex and that the exposure time is much longer (2 or 3 h) which makes it impossible to measure diffraction of a reactive sample, which degenerates with time, or to perform kinetic studies.

angle of 20° can be easily measured. Since the possible energy of the incident X-ray beam at ID27 of ESRF is very high (up to 90 keV) (Mezouar *et al.*, 2005), such a small cone can in fact cover a sufficient wide range of *d*-values (down to 0.4 Å) in spite of the limited X-ray access. These grooves are also made in the other side for the incident beam, allowing (by rotating the cell around the vertical axis and recording only half image plates) a 2θ angle up to 40° (the coverage in *d*-spacing is hence theoretically up to 0.2 Å, enough to allow robust structural refinement). Moreover, as already outlined, to be able to perform angular-dispersive X-ray diffraction a Sollers slits system has to be used to eliminate most of the background signal coming from the sample environment. Since the efficiency of such a system is better when the first set of slits is as near as possible to the sample, grooves were made in the first-stage anvils in order to bring the Sollers slit system closer to the sample (see Fig. 3). The Sollers slit system therefore penetrates inside the anvils, as shown in Fig. 4, allowing a better collimation of the diffracted beam. All these modifications did not lead to noticeable deterioration of the (P, T) performance of our apparatus.

3.3.2. Modifications of the second-stage anvils. This second stage is assembled outside the press and consists of eight cubes of 10 mm edge length, usually made of WC for *ex situ* studies. However, recent industrial developments have provided large-size sintered cubic boron nitride (cBN) as an alternative anvil material. cBN is an ultra-hard material, in fact the third hardest material after diamond and cubic BC_2N. Consequently, by replacing the WC with cBN, an extension of the achievable pressure has been demonstrated. However, the main advantage of the cBN is its transparency to X-rays. Hence, for *in situ* X-ray diffraction experiments the diffracted beam from the sample easily passes through the second-stage anvil, allowing the collection of data in the angle-dispersive measurements. The only problem with this adaptation is related to the passage of the electrical current up to the furnace in the interior of the octahedron. Heating is accomplished by passing an electrical current from one cube through the electrical contacts, the heater and out through the opposite cube, *i.e.* two cubes act as contacts for the heater. Owing to the cobalt binder, there was no problem with conductivity of the WC cubes, but cBN is a large-gap (6.2 eV) semiconductor. First we attempted to use finely cut-out copper strips to connect the electrical contacts on the octahedron to the first-stage anvil. However, because of the large flow of gasket material between the cubes, these metal sheets often break. This problem was avoided by using two WC cubes (out of the beam) and six cBN cubes for the X-ray diffraction beam path.

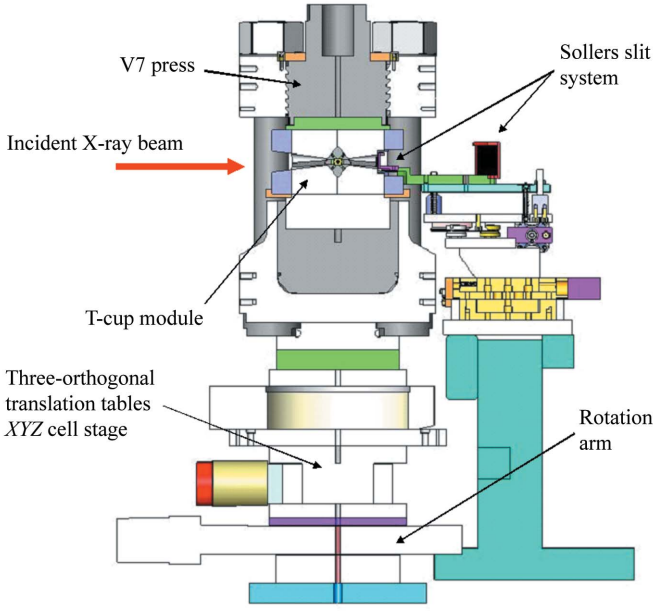

Figure 4
Schematic drawing of our apparatus interfaced with the Sollers slit system in the ID27 X-ray hutch.

3.3.3. Modifications of the sample environment. In the octahedron, the most absorbing material at all wavelengths is the lanthanum chromate heater. Of course, disc-heater cells allowing X-ray access to the sample are quite familiar in various multi-anvil apparatus combined with synchrotron diffraction. Nevertheless, it is also well known that such geometries in plates appreciably increase the thermal gradients within the sample.

To preserve a cylindrical geometry, the use of refractory metal furnaces is necessary. In this case the lower intrinsic resistivities of these metals should be compensated by a very low thickness in order to keep a sufficient value for overall resistance. Moreover, the general rule is that resistivity increases with increasing temperature in metals and decreases in $LaCrO_3$ or graphite. This means that, contrary to these usual furnaces, if a hot point appears in the metallic furnace because of imperfections or an incorrect flow of the set-up, this hot point will raise its resistance and hence will increase its temperature again, causing a self-sustained mechanism and thus finally explosions. We first attempted to replace the chromate heater with a rhenium foil of thickness 12.5 µm but such a cell design has been found to be very unstable at high temperatures, causing several blow-outs for temperatures exceeding 1200 K.

By increasing the thickness of such a metallic furnace from 12.5 µm to 25 µm, the stability of the heating system is much better and no furnace failure has been found up to 2000 K. Above this value, for reasons not yet well known, new instabilities appear which could be attributed to the insufficient thermal insulation in our cell.

The main advantage of this heater design, however, is its transparency to X-rays. It allows X-rays to pass through the octahedron since the absorption of 50 µm (25 µm on each side) of Re is only about 48% at 50 keV or 24% at 70 keV, easily compensated by the elevated brightness of the ESRF beamline ID27 (Mezouar *et al.*, 2005).

Fig. 5 shows the sample assembly most often used for *in situ* X-ray diffraction studies at the ESRF.

To resume, it is possible to use our portable multi-anvil press combined with optimized Sollers slits and large-area CCD detectors for angle-dispersive X-ray diffraction. Fig. 6 shows the device installed at beamline ID27 of the ESRF. This

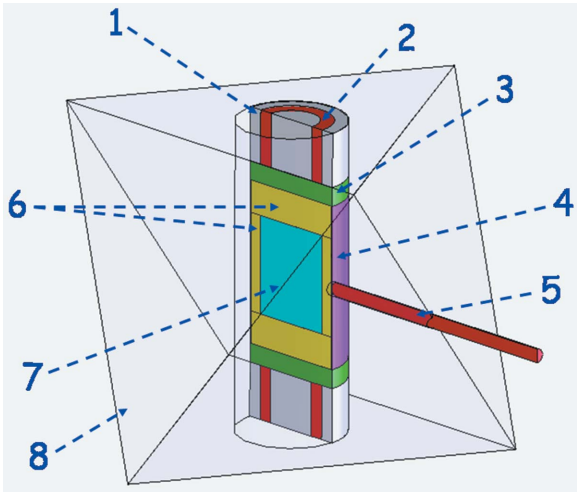

Figure 5
Sample assembly used for *in situ* synchrotron X-ray diffraction study. (1) Insulating ceramic. (2) Electrical contact. (3) Molybdenum disc. (4) Furnace (Re). (5) Thermocouple. (6) Sample capsule (usually MgO). (7) Sample. (8) Octahedron.

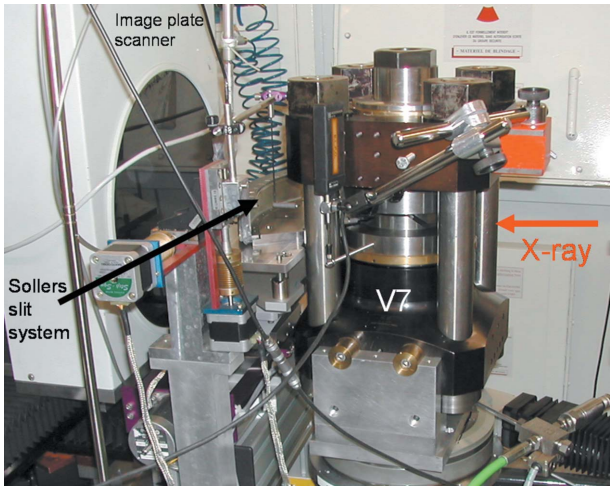

Figure 6
Photograph of the device installed at beamline ID27 at the ESRF. The incident beam of synchrotron radiation comes from the right and the image-plate detector is seen on the left.

combination of our apparatus with a Sollers slits system permits a significant improvement of the signal-to-background ratio and provides clean diffraction patterns of crystalline, amorphous and even liquid samples as will be demonstrated below.

4. Experimental methods

4.1. Monochromatic diffractometer at ID27

The angle-dispersive X-ray geometry used at ID27 at the ESRF has been fully described previously (Mezouar *et al.*, 2005). A very intense monochromatic beam is selected using a nitrogen-cooled silicon (111) monochromator and highly focused on the sample using multilayer mirrors in the Kirkpatrick–Baez geometry. The dimensions of this monochromator are optimized to select a broad energy range up to 90 keV which is largely sufficient for high-pressure diffraction experiments. The primary monochromatic synchrotron beam is then collimated down to 100 µm (width) × 200 µm (height) by two sets of WC slits and, because of the (111) geometry of our apparatus, is perpendicular to the vertical axis of the sample chamber.

Our portable multi-anvil apparatus is mounted on a three-orthogonal translation tables *XYZ* cell stage and a rotation arm with a rotation centre that coincides with the vertical axis of the press. This allows micro-positioning of the sample to an accuracy of better than 10 µm. The set-up is also equipped with a photodiode mounted on a pneumatic actuator that moves it in and out of the X-ray beam. This photodiode, located between the multi-anvil cell and the image-plate detector, is used for the initial centring of the sample[3] as well as for rapid checking of the alignment after each compression.

The diffracted beam is collimated by a Sollers slit system (Mezouar *et al.*, 2002), installed on a *yz* translation that permits alignment of the central slit on the incident beam. This multi-channel collimator is made of two concentric sets of slits. The inner and outer slits are located 50 and 200 mm, respectively, from the sample. The inner slits (made from a single block of tantalum), of width 100 µm and angular separation 0.8°, are designed in order to minimize the volume seen by the two-dimensional detector and maximize the signal detected. The outer-slit widths are fixed at 300 mm which is sufficient to ensure an excellent signal-to-noise ratio. These back slits are made from a Pb–Sb alloy. The two sets of slits are mechanically aligned with high precision on a base plate that supports the slit system. This base plate is made of Invar to prevent any variation of the system dimensions in the case of temperature fluctuation in the experimental hutch. Proper alignment of this multi-channel is crucial, and Crichton & Mezouar (2005) explain in detail the standard alignment procedure, which is very fast at ID27 and never exceeds 10 min. Angle-dispersive data are collected using a MAR345 image-plate scanner, a device which has a large input surface of more than 150 mm diameter, a high spatial resolution, low noise and high dynamic range, as well as a good sensitivity at high X-ray energies above 30 keV. The precise calibration of the sample-to-detector distance is usually made prior to the high-pressure experiment by measuring a NBS LaB_6 (Standard Reference Material 660a) powder. Exposure times are typically between 60 and 150 s depending on the electron current. Integrations of the two-dimensional diffraction images corrected for spatial distortions are performed using the *FIT2D* software (Hammersley *et al.*, 1996).

4.2. *P*, *T* generation and metrology

During the diffraction experiments, the pressure is easily determined using a pressure marker such as MgO (used, for

[3] The first alignment is made with an absorbing steel second-stage anvil of substitution, finely bored in its centre to simulate the passage of the beam and by a laser that delineates a rough beam path.

example, as a sample capsule, see Fig. 5) or Re in conjunction with their equations of state.

The sample temperature is measured using a W3%Re97%–W25%Re75% thermocouple (for experiments where the pressure does not exceed 12 GPa), or (for higher pressure) with a coaxial platinum–rhodium (type B) or chromel–alumel (type K) thermocouple in contact with the furnace (Fig. 5), with no correction for the pressure effect on the thermocouple electromotive force. In the case of thermocouple failure, the sample temperature can be estimated by an established power–temperature relation or by the double isochors method (Crichton & Mezouar, 2002), though the accuracy is poorer.

In our system, the temperature can be fixed almost immediately, contrary to the pressure. It is well known that multi-anvil systems of any kind are very sensitive to the rate of compression or decompression. In our experiment, the rate of compression is typically 2 GPa h^{-1} for the first 4 GPa and beyond this stage becomes faster, about 10 GPa h^{-1}. On the other hand, the rate of decompression is known to be very important for the survival of the second-stage anvils. In our case, we usually decompress to ambient conditions at a typical speed of 2 GPa h^{-1}. In principle, this decompression is not interesting and no diffraction data are recorded during this procedure. Hence, this long decompression time (several hours) usually leads to a considerable loss of beam time. This is a well known and non-negligible inconvenience of the use of conventional (non-compact) presses to operate multi-anvil devices. In our case, our apparatus being portable, we are in a position to work with several presses simultaneously, *i.e.* carry out experiments with one cell whereas other presses are being prepared for the following measurements. In our recent experiments at ID27, we have, in fact, operated using two V7 cells simultaneously. So, by quickly removing the press (where the sample under study is at high pressure) of the experimental hutch, the decompression of a finished experiment is made off-line while a new experiment starts with the other press.

The rate of compression and decompression has been optimized for the survival of the cBN cubes. The survival rate of the latter is reasonably good, with anvils only damaged after experiments under very severe conditions (for example, for experiments with long heating times at the highest temperatures and pressures). Blow-outs are, in fact, rare and occur exclusively during compression where a large volume-changing phase transition takes place in the sample or with anvils which were already internally damaged during a previous experiment.

5. Examples

In the following section, some angle-dispersive diffraction studies performed with our new apparatus are discussed. This will illustrate the quality of the data which can be collected with this device and the potential application of the technique.

5.1. Oxides under extreme conditions

One of the common points in the following studies is to determine the high-pressure crystallographic structure of oxide compounds. If this task seems to be straightforward at first sight, the associated experimental difficulties are often considerable as much care must be taken in the peak assignment. In fact, it is often very difficult to establish unambiguously whether a structural transition has taken place within a single-phase material since new peaks could be due to (i) scattering from the sample assembly (which can strongly be deformed under pressure), (ii) chemical reactions with the sample environment, (iii) reduction of the sample because of the low oxygen fugacity in the high-pressure cell and (iv) phase dissociation.

5.1.1. Magnetite Fe_3O_4. Magnetite (Fe_3O_4) crystallizes under ambient conditions in the cubic spinel structure with space group *Fm3m* (eight formula units per unit cell). Under pressure it transforms beyond ~25 GPa into the orthorhombic $CaMn_2O_4$ structure (*Pbcm*) (Fei *et al.*, 1999) or the closely related $CaTi_2O_4$ structure (*Bbmmm*) (Haavik *et al.*, 2000; Dubrovinsky *et al.*, 2003). All accurate diffraction data available so far were obtained in diamond anvil cells and show that heating is crucial for obtaining single-phase material and sharp diffraction lines. In Fig. 7 we show a diffraction pattern of the spinel phase which allows us to assess the data quality obtained by the set-up. The powder sample was obtained by grinding part of a large natural single crystal of Fe_3O_4 purchased from NEYCO. The pattern corresponds to a load of 110 ton and a temperature of 570 K, derived *a posteriori* through a calibration of the injected power (75 W). Initial refinements were carried out using only the spinel structure but the small reflections at 5.3 and 6.5° indicate a minor amount of hematite Fe_2O_3 which was already present under

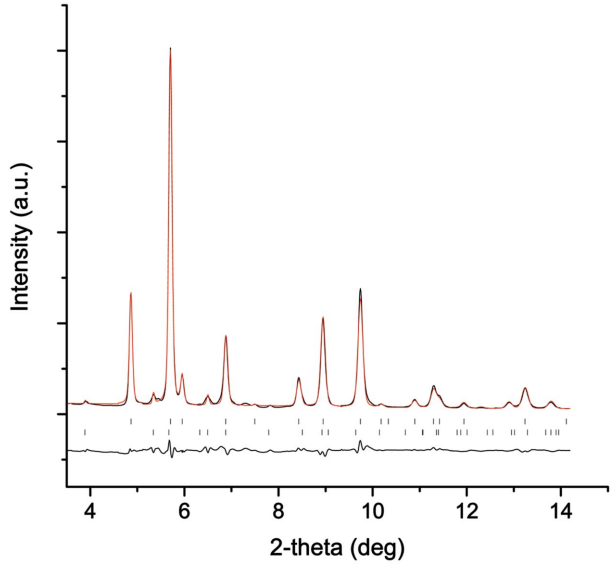

Figure 7
Diffraction pattern of Fe_3O_4 (raw data) at 16.3 GPa and 570 K. The top line is a Rietveld fit through the data; the difference curve is given below. The small reflections at 5.3 and 6.5° are due to a small amount of hematite which was included in the fit (lower tickmarks). λ = 0.246 Å.

ambient conditions. Including this phase in the refinements and varying the lattice parameters, the internal oxygen coordination z(O) of Fe_3O_4, two thermal and three profile coefficients for magnetite gives a = 8.19390 (3) Å and z(O) = 0.25849. The unit-cell volume indicates a pressure of 16.3 GPa based on a Birch–Murnaghan equation of state with a_0 = 8.392 Å (300 K), B = 186 GPa and B' = 4 (Finger *et al.*, 1986) and a thermal expansion of 2.06 × 10^{-5} K^{-1} (Skinner, 1966). A similar analysis using the refined unit-cell volume of the hematite impurity (V = 285.8 $Å^3$) with corresponding parameters B = 230 GPa, B' = 3.5 (Finger & Hazen, 1980) and α = 2.4 × 10^{-5} K^{-1} (Skinner, 1966) gives P = 15.0 GPa. These pressure values are somewhat lower compared with those expected from the empirical load/pressure relation using BN anvils. The internal oxygen coordinate of magnetite is somewhat larger than that found under ambient conditions, *i.e.* z(O) = 2.550 (Wright *et al.*, 2002), but the difference is probably not significant. Upon increasing the temperature to 600 K at constant load the sample spontaneously transformed into probably a multiphase compound and the data are currently being analyzed. Overall, this example demonstrates that clean diffraction patterns can be obtained with this set-up under HP-HT conditions which are readily refinable using Rietveld techniques.

5.1.2. $CuGaO_2$. $CuGaO_2$ belongs to the delafossite $CuMO_2$ family (M = Al, Ga or In) which are transparent conducting oxides with potential optoelectronic applications owing to their p-type or bipolar (for M = In) conductivity. The crystal structure under ambient conditions is rhombohedral (space group $R3m$), with four atoms in the primitive cell, which can be described as a triple hexagonal cell, with Cu and Ga cations occupying, respectively, 3(a) (0,0,0) and 3(b) (0,0,1/2) Wickoff positions and O atoms are situated in 6(c) (0,0,u) positions. The oxygen coordination is very different for the two cations. The Ga cation is in octahedral coordination, whereas Cu forms linear O—Cu—O bonds and is hence only twofold coordinated. This difference in cation coordination suggests a rich high-pressure behaviour. Recent structural and vibrational measurements under pressure performed in diamond anvil cells have shown the occurrence of an irreversible phase transition around 25 GPa at room temperature (Pellicer-Porres *et al.*, 2004, 2005). The transition pressure decreases slightly by increasing temperature. Nevertheless, the structure of the high-pressure phase remains unknown. In order to explore the (P,T) phase diagram of $CuGaO_2$ we performed an experiment using our set-up. Diffraction patterns were recorded at 16 GPa at increasing temperatures. As shown in Fig. 8, high-quality spectra have been obtained. Reflections from the $CuGaO_2$ sample have been clearly identified and indexed. Only a few peaks from boron (low angle) and MgO are superimposed. As occurred for magnetite, upon increasing the temperature to 680 K at 16 GPa, the sample partly decomposed, and at least $CuGaO_2$ and Ga_2O_3 peaks have been identified, but other phases are present and data are currently being analyzed.

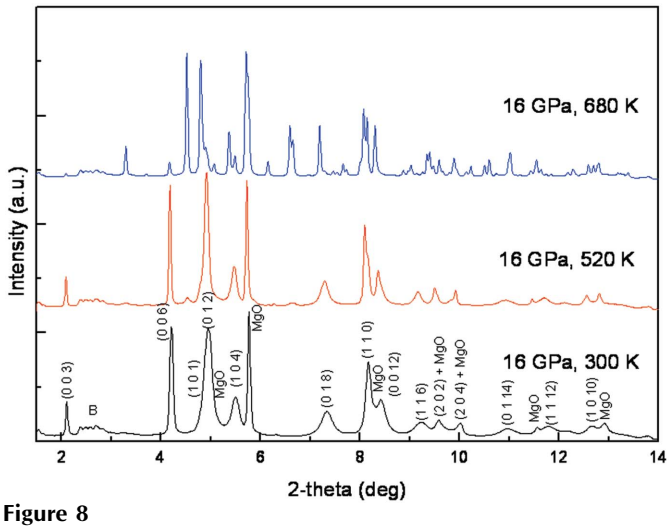

Figure 8
Diffraction patterns of $CuGaO_2$ at 16 GPa at increasing temperatures.

5.2. Possible HP-HT synthesis of new super-hard materials

While diamond exhibits extreme hardness, its performance as a super-abrasive is somewhat limited. It is not stable in the presence of oxygen even at moderate temperatures, nor is it a suitable abrasive for machining ferrous alloys. cBN exhibits higher thermal stability and is the super-abrasive of choice for working with steels, but has only half the hardness of diamond. A possible solution is to synthesize diamond-like binary or ternary phases containing second-row elements (B, C, N, O) since these materials might be more thermally and chemically stable than diamond, and harder than cBN, and thus be an excellent material for high-speed cutting and polishing of ferrous alloys.

The conditions normally employed to synthesize super-hard materials require extreme pressures and temperatures. Consequently, fundamental research on the subject is lacking, especially research on novel diamond-like phases in the B–C–N–O system.

Our large-volume multi-anvil system at ESRF will provide a unique capability to tackle the synthesis and characterization of new high-pressure phases of the B–C–N–O system that was not previously available to researchers in this area. Two preliminary results could be mentioned here.

(i) Recently we have studied *in situ* the HP-HT behaviour of cyanoguanidine $C_2N_4H_4$ that has been claimed as a possible precursor for the hypothetical ultra-hard phase of C_3N_4 (Horvath-Bordon, 2004). We have found that this compound becomes amorphous already at relatively low pressures and remains amorphous up to 20 GPa and 1000 K without formation of any new phase. However, further studies at higher temperatures and pressures are required to make definite conclusions on the prospects of this precursor for synthesis of ultra-hard C–N phases.

(ii) Very recently we have studied the chemical interaction between β-rhombohedral boron and hexagonal boron nitride (hBN) at 7.4 GPa and 1973 K in order to clear the situation

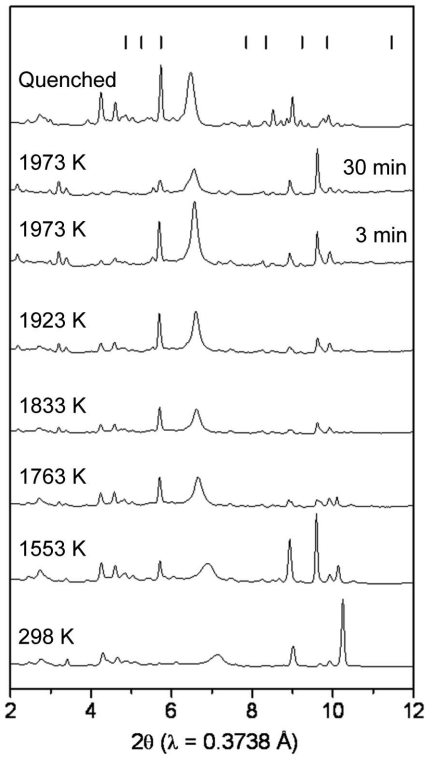

Figure 9
Sequence of the X-ray diffraction patterns collected *in situ* during the stepwise heating of the B–BN mixture at 7.4 GPa. The bars on the top represent the expected line positions for the hypothetical B_6N phase with B_6O-like structure [$R3m$, a = 5.457 Å, c = 12.241 Å (Hubert *et al.*, 1997)].

with solid-state synthesis of boron subnitride B_6N reported earlier in the literature (Hubert *et al.*, 1997).

Fig. 9 shows the set of the diffraction patterns obtained *in situ* during the heating of the boron–hBN mixture of the 'B_6N' stoichiometry at 7.4 GPa. The details are described elsewhere (Solozhenko *et al.*, 2006). No interaction occurs in the mixture; only the random change in relative intensities of various boron reflections is observed. During the 30 min heating at 1973 K, the boron reflections do not disappear and the expected B_6N reflections do not arise. At the same time, HP-HT treatment has resulted in strong and unpredictable preferred orientation of boron crystallites. This leads to the rise of some weak boron reflections that might be erroneously attributed to the appearance of a new phase.

In the powder diffraction pattern of the quenched sample we do not see lines consistent with the pattern of B_6N, although some reflections of boron have the same position as the reflections of hypothetical B_6O-like boron subnitride.

Thus, the results of our *in situ* studies have allowed us to conclude that the evidence for the solid-state synthesis of boron subnitride B_6N with B_6O-like structure reported by Hubert *et al.* (1997) is inconclusive, and much higher temperatures are probably required to enable chemical interaction in the B–BN system.

It is worthy of notice that the quality of all diffraction data was excellent, despite the samples being composed of the low-Z elements.

5.3. Liquid under extreme conditions

X-ray diffraction on liquids gives access to the average local order. Liquids, like amorphous materials, are characterized by a short-range order. Liquid metallic alloys are organized in clusters (~60 Å) with an arrangement intimately linked to the structure of the corresponding solid (Kumar, 1968). Structural and electronic transitions that take place in the solid phase could also happen in the liquid state (Brazhkin *et al.*, 1997).

Sulfur might be the major light element alloyed with iron to form Mars' core (Sohl & Spohn, 1997). It could also be present in the Earth's core, but in lower content (1.7 wt% S). Sulfur strongly modifies the local average structure of the pure liquid iron, and provokes an important decrease in the compressibility (Sanloup *et al.*, 2002). We show here investigation of the structural evolution of the Fe–FeS eutectic liquid at high pressure. Details will be published elsewhere.

X-ray angle-dispersive scattering was performed on a fine mixture of pure Fe powder (99.9%, GoodFellow) and pure FeS powder (99.9%, Alfa Aesar), following the eutectic composition [19 wt% S at 15 GPa (Fei *et al.*, 1997)]. For this study, the furnace set-up was different than previously presented in §2. In order to reduce the absorption of the sample environment, the furnace was composed of two 25 µm-thick Re strips disposed laterally (*i.e.* out of the beam path) with respect to the X-ray beam. A hole of diameter 1 mm and depth 1 mm was drilled into a MgO polycrystalline capsule.

Synchrotron radiation from two undulators was monochromated by a Si(111) double crystal. The energy of the X-ray beam was 71.7 keV (λ = 0.17298 Å, Re *K*-edge) for the liquid scattering patterns.

During the experiment, the pressure was increased up to 15 GPa, then the temperature was raised by steps of 20 W at a rate of 5 W min^{-1}. The observation of diffuse rings with the simultaneous disappearance of solid-phase diffraction peaks was the criterion used to assess the complete melting of the sample.

The study of the liquid structure needs high-quality signal. A large-volume sample is required in order to have an intense signal from the liquid. Furthermore, the Sollers slits system increases the liquid-signal/capsule-signal ratio with increasing angle. In our case, the contribution to the total signal from the capsule begins to decrease around 5° and is completely removed for angles superior to 17°. The contribution of the MgO capsule can be easily removed by fitting the liquid signal, using the part where its contribution is evident (Fig. 10*a*). It should also be noted that FeO diffraction peaks appeared owing to a reaction between water remaining in the capsule and the sample.

Then, normalization and Fourier transform procedures (Eggert *et al.*, 2002) could be performed in order to extract structural information using the pair distribution function $g(r)$ (Fig. 10*b*). Contrary to what is found at lower pressures, the radial distribution function clearly resembles that of a random close-packed (r.c.p.) structure. The data hence show that, for pressures beyond 15 GPa, liquid iron is able to insert sulphur while maintaining an r.c.p. structure (Morard *et al.*, 2009),

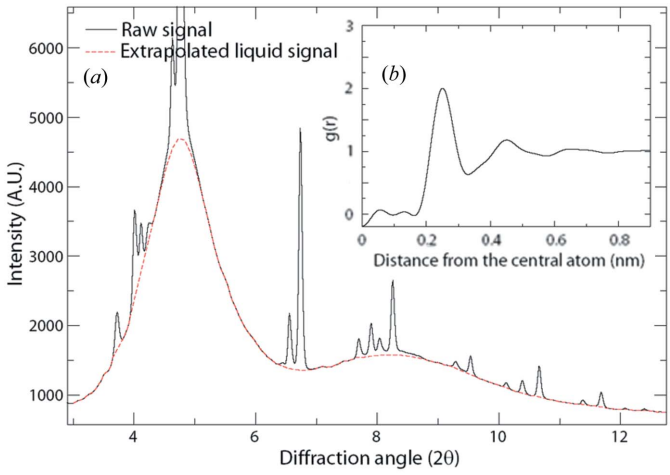

Figure 10
(*a*) Angle-dispersive *in situ* X-ray scattering pattern of the Fe–FeS eutectic liquid at high pressure and high temperature and its corresponding fit. The remaining diffraction peaks belong to MgO, the pressure medium, and to FeO, owing to reaction between water remaining in the capsule and the sample. (*b*) Radial distribution function $g(r)$ extracted from the liquid X-ray scattering pattern.

indicating that sulfur has a lower destabilizing effect on the liquid structure. Detailed analysis of this study will be published elsewhere but these results clearly open the door towards the collection of high-quality data of liquid or amorphous materials with our new apparatus at high pressure and high temperature.

6. Future developments

We intend to further increase the performance of our system in the near future and to transfer our new method to other types of *in situ* experiments. Only three issues will be discussed here, corresponding to developments which are currently in progress: (i) extension to higher pressures, (ii) extension to higher temperatures, and (iii) brief description of new *in situ* characterizations at HP-HT that will be carried out using this portable multi-anvil cell.

6.1. Higher pressures

The hardness of the anvil materials is of course the main key factor in the attainable pressures in our high-pressure apparatus if the gasket and the pressure medium are fully optimized. The Knoop hardness of cBN is generally in the range 40–45 GPa, while that of diamond (of gem quality) is ~100 GPa. Hence, the use of sintered diamond anvils instead of cBN, with a similar profile, is expected to increase substantially the maximal pressure. Recently, large-size sintered diamond anvils have become commercially available and these anvils proved to be hard enough for the generation of pressures up to 40 GPa with the usual 7/2 configuration. Nevertheless, it has been reported also that blow-outs frequently occur, rendering the use of such anvils very expensive for routine experiments (about USD 1000 per piece for a cube with an edge length of 10 mm).

Another much less expensive option consists of further reducing the sample volume. Very recently, high-pressure generation using an octahedral assembly with 5 mm edge length has been reported up to 69 GPa (at room temperature) in a multi-anvil system with 1.5 mm corner truncation cubes (Ito *et al.*, 2004). In this new sample assembly, called 5/1.5, the sample is quite smaller. Therefore, and hence, a new Sollers slits system is currently being developed at ESRF where the width of the inner slits is 70 µm instead of 100 µm in order to keep a good collimation for the diffracted beam.

6.2. Higher temperatures

A number of changes are needed to extend the limits of temperature. The first problem is the rhenium furnace since the temperature is restricted by its instability at high pressure and temperature. We are currently testing a new cylindrical furnace made of TiC, which has been previously powder-compacted. This material, which has already been utilized in many HP-HT methods, could increase the temperature range (up to 2500 K) without a major change in the geometry of the current design. Nevertheless, a better thermal insulation in our cell will also be necessary in order to reach these higher temperatures and minimize the thermal gradients in our sample. For that, a new sample assembly with $LaCrO_3$ discs replacing those made of molybdenum in Fig. 5 has recently proven to be very useful. At the same time, we are aiming to investigate the efficiency of a new cooling system that we developed recently for the first-stage anvils.

6.3. Other possible *in situ* applications at HP-HT

Our portable multi-anvil cell should be quickly transferred to other methods of *in situ* characterization under extreme conditions, in the same way as that of the standard PE cell during recent years. A set-up for the ultrasonic measurement of elastic properties of single crystals or polycrystalline samples at high pressure with our apparatus has been tested. In order to adapt our cell for ultrasonic measurements, the first-stage anvil profile has been modified to allow the mounting of a transducer onto the rear face of one second-stage anvil cube, previously flattened and polished, which serves as an acoustic buffer rod to transmit the high-frequency signals into the cell assembly (Fig. 11). Coupled with X-ray diffraction, this technique could enable determination of the elastic properties and their pressure derivatives.

Another possibility is to adapt our set-up for X-ray absorption spectroscopy (XAS) experiments. The use of large-volume cells instead of diamond anvil cells for XAS measurements at high pressure and temperature has several advantages. On one hand, the problem of diamond Bragg peak rejection is overcome and classical step-by-step XAS in both transmission or fluorescence mode becomes possible. On the other, the sample size is larger and the pressure and temperature homogeneity better than in diamond anvil cells, allowing the use of focusing double monochromators with large spot size, which improves the signal-to-noise ratio. As a matter of fact, experiments at high pressure (up to 6 GPa) and

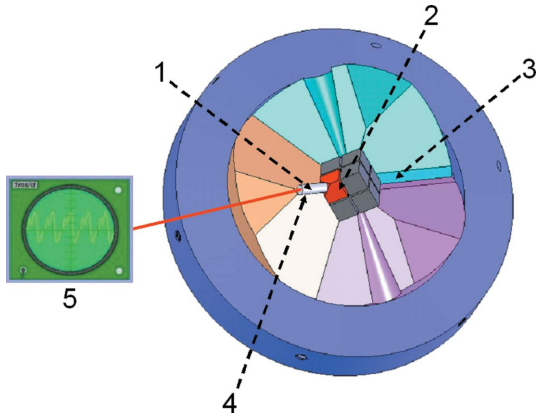

Figure 11
Schematic diagram of the modified T-cup module for ultrasonic studies. (1) Transducer. (2) WC cube with transducer attached to the back. (3) and (4) New grooves into the first-stage anvils allowing a better passage of the transducer to the second-stage anvils. (5) Oscilloscope.

temperature (up to 1000 K) using classical XAS with a double monochromator coupled to step-by-step energy-dispersive or angular-dispersive X-ray diffraction has been successfully performed in recent years with the PE press (Filipponi *et al.*, 2003; Principi *et al.*, 2006). An extension of the pressure and temperature range using our multi-anvil set-up will allow the use of XAS techniques to study high-density liquids as well as solid phases present for example in the upper mantle of the Earth.

The work reported in this paper is supported by the French 'Réseau Hautes Pressions', the 'Mission Ressources et Compétences Technologiques' of the CNRS and the University Pierre & Marie Curie, as well as the 'Agence Nationale de la Recherche' through grant No. NT05-3_42601. High-pressure experiments have been carried out during beam time allocated to proposal HS-2532 at ID27, ESRF. We are grateful to Olexander Kurakevych and Raul Lacomba for their help in the X-ray diffraction measurements.

References

Besson, J. M., Nelmes, R. J., Hamel, G., Loveday, J. S., Weill, G. & Hull, S. (1992). *Physica B*, **180**, 907–910.
Brazhkin, V. V., Popova, S. V. & Voloshin, R. N. (1997). *High Press. Res.* **15**, 267–305.
Brister, K. (1997). *Rev. Sci. Instrum.* **68**, 1629–1647.
Crichton, W. A. & Mezouar, M. (2002). *High Temp. High Press.* **34**, 235–242.
Crichton, W. A. & Mezouar, M. (2005). *Advances in High-Pressure Technology for Geophysical Applications.* Amsterdam: Elsevier.
Dubrovinsky, L. S., Dubrovinskaia, N. A., McCammon, C., Rozenberg, G. K., Ahuja, R., Osorio-Guillen, J. M., Dmitriev, V., Weber, H. P., Le Bihan, T. & Johansson, B. (2003). *J. Phys. Condens. Matter*, **15**, 7697–7707.
Eggert, J. H., Weck, G., Loubeyre, P. & Mezouar, M. (2002). *Phys. Rev. B*, **65**, 174105.
Fei, Y., Bertka, C. M. & Finger, L. W. (1997). *Science*, **275**, 1621–1623.
Fei, Y., Frost, D. J., Mao, H. K., Prewitt, C. T. & Häusermann, D. (1999). *Am. Mineral.* **84**, 203–206.
Filipponi, A., Giordano, V. M., De Panfilis, S., Di Cicco, A., Principi, E., Trapananti, A., Borowski, M. & Itié, J. P. (2003). *Rev. Sci. Instrum.* **74**, 2654–2664.
Finger, L. W. & Hazen, R. M. (1980). *J. Appl. Phys.* **51**, 5362–5368.
Finger, L. W., Hazen, R. M. & Hofmeister, A. M. (1986). *Phys. Chem. Miner.* **13**, 215–220.
Haavik, C., Stølen, S., Fjellvåg, H., Hanfland, M. & Häusermann, D. (2000). *Am. Mineral.* **85**, 514–524.
Hammersley, A. P., Svensson, S. O., Hanfland, M., Fitch, A. N. & Häusermann, D. (1996). *High Press. Res.* **14**, 235–248.
Horvath-Bordon, E. (2004). PhD thesis, TU Darmstadt, Germany.
Hubert, H., Garvie, L. A. J., Busec, P. R., Petuskey, W. T. & McMillan, P. F. (1997). *J. Solid State Chem.* **133**, 356–369.
Huppertz, H. (2004). *Z. Kristallogr.* **219**, 330–338.
Irifune, T. (2002). *Mineral. Mag.* **66**, 769–790.
Ito, E., Kubo, A., Katsura, T. & Walter, M. (2004). *Phys. Earth Planet. Int.* **143–144**, 397–406.
Kawaii, N. & Endo, S. (1970). *Rev. Sci. Instrum.* **41**, 1178–1181.
Klotz, S., Besson, J. M., Hamel, G., Nelmes, R. J., Loveday, J. S., Marshall, W. G. & Wilson, R. (1995). *Appl. Phys. Lett.* **66**, 1735.
Kubo, T., Ito, E., Katsura, T. Shinmei, T., Yamada, H., Nishikawa, O., Song, M. & Funakoshi, K. (2003). *Geophys. Res. Lett.* **30**, doi:10.1029/2002GL016394.
Kumar, R. (1968). *Liquids, A Contemporary Physics Reprint.* London: Taylor and Francis.
Le Godec, Y., Hamel, G., Martinez-Garcia, D., Hammouda, T., Solozhenko, V. L. & Klotz, S. (2005). *High Press. Res.* **25**, 243–253.
Le Godec, Y., Solozhenko, V. L., Klotz, S. & Mezouar, M. (2008). *Actual. Chim.* **322**, 27–34.
Mezouar, M., Crichton, W. A., Bauchau, S., Thurel, F., Witsch, H., Torrecillas, F., Blattmann, G., Marion, P., Dabin, Y., Chavanne, J., Hignette, O., Morawe, C. & Borel, C. (2005). *J. Synchrotron Rad.* **12**, 659–664.
Mezouar, M., Faure, P., Crichton, W. A., Rambert, N., Bauchau, S. & Blattmann, G. (2002). *Rev. Sci. Instrum.* **73**, 3770–3774.
Morard, G., Sanloup, C., Fiquet, G., Mezouar, M., Rey, N., Poloni, R. & Beck, P. (2007). *Earth Planet. Sci. Lett.* **263**, 128–139.
Pellicer-Porres, J., Segura, A., Ferrer-Roca, Ch., Martínez-García, D., Sans, J. A., Martínez, E., Itié, J. P., Polian, A., Baudelet, F., Muñoz, A., Rodríguez-Hernández, P. & Munsch, P. (2004). *Phys. Rev. B*, **69**, 024109.
Pellicer-Porres, J., Segura, A., Martínez, E., Saitta, A. M., Polian, A., Chervin, J. C. & Canny, B. (2005). *Phys. Rev. B*, **72**, 064301.
Principi, E., Minicucci, M., Di Cicco, A., Trapananti, A., De Panfilis, S. & Poloni, R. (2006). *Phys. Rev. B*, **74**, 064101.
Sanloup, C., Guyot, F., Gillet, P. & Fei, Y. (2002). *J. Geophys. Res.* **107**, 2272–2282.
Shimomura, O. (1984). *J. Miner. Soc. Jpn*, **16**, 423–433.
Skinner, B. J. (1966). *Handbook of Physical Constants*, edited by S. P. Clark. Geological Society of America Memoir.
Sohl, F. & Spohn, T. (1997). *J. Geophys. Res.* **102**, 1613–1635.
Solozhenko, V. L., Andrault, D., Fiquet, G., Mezouar, M. & Rubie, D. C. (2001). *J. Appl. Phys.* **78**, 1385–1388.
Solozhenko, V. L, Kurakevych, O. O., Andrault, D., Le Godec, Y. & Mezouar, M. (2009). *Phys. Rev. Lett.* **102**, 015506.
Solozhenko, V. L., Le Godec, Y. & Kurakevych, O. O. (2006). *C. R. Chim.* **9**, 1472–1475.
Vaughan, M. T., Weidner, D. J., Wang, Y., Chen, J., Koleda, C. C. & Getting, I. C. (1998). *Rev. High Press. Sci. Technol.* **7**, 1520–1522.
Wang, Y., Uchida, T., Von Dreele, R., Rivers, M. L., Nishiyama, N., Funakoshi, K., Nozawa, A. & Kaneko, H. (2004). *J. Appl. Cryst.* **37**, 947–956.
Wright, J. P., Attfield, J. P. & Radaelli, P. G. (2002). *Phys. Rev. B*, **66**, 214422.